Accepted Manuscript

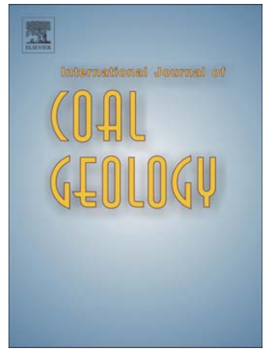

Horizontal stress anisotropy and effective stress as regulator of coal seam gas zonation in the Sydney Basin, Australia

Agi Burra, Joan S. Esterle, Suzanne D. Golding

PII: S0166-5162(14)00181-5
DOI: doi: 10.1016/j.coal.2014.08.008
Reference: COGEL 2358

To appear in: *International Journal of Coal Geology*

Received date: 26 May 2014
Revised date: 12 August 2014
Accepted date: 12 August 2014

Horizontal stress anisotropy and effective stress as regulator of coal seam gas zonation in the Sydney Basin, Australia

Agi Burra, Joan S. Esterle, Suzanne D. Golding

School of Earth Sciences, University of Queensland, QLD 4072, Australia

Corresponding author email: agi@spemail.org

Abstract

Coal seam gas zonation in the Sydney Basin, NSW, Australia is related to basin hydrodynamics and hydrochemical facies evolution along the flow path from the subcrop to the basin centre. Biogenic methane corresponds with meteoric water under hydrostatic pressure and persists down to the top of the geopressured zone (~800 - 1000m). Thermogenic gases, including wet hydrocarbons, can reach up to relatively shallow horizons of less than 500 - 600m depth. In the transition zone between the top of the geopressured and base of the hydrostatic zone, a mixed water and gas regime prevails, comprising brackish waters, and gases of mixed biogenic, thermogenic and inorganic origins, including CO_2. Mechanisms for and the role of stress in the development of this layered hydrogeological and gas environment are investigated in this paper.

The inverse relationship between effective horizontal stress and permeability in coals through regulation of cleat volumes is well documented, and there is evidence of regionally compartmentalised stress regimes with depth within the Sydney and other eastern Australian coal basins. This regional stress regime can be overprinted by the effect of localised geological features. It is hypothesised that the *in situ* stress regime plays an important role in the regulation of groundwater flow regimes and extents, resulting in the development of the reported gas content and compositional zonation.

Analysis of regional gas and stress data obtained from public and private databases, as well as literature, supports this hypothesis. Changes in gas concentration and composition with depth correspond with discernable variations in horizontal stress anisotropy. Gas contents generally increase with depth down to a 'peak gas' horizon, below which concentrations decrease. This 'peak gas' zone is coincident with a horizontal stress anisotropy change from moderately high to low levels, associated with reverse to strike-slip faulting conditions, respectively. The stress release zone also marks the top of the thermogenic gas zone, identified by the first appearance of ethane in the vertical profile. This zone also hosts gases of mixed origins: biogenic, thermogenic and inorganic (CO_2) and represents a mixed (transitional) groundwater flow environment. The base of the mixed gas zone is the top of the 'geopressured-only' flow associated with thermogenic gases and is signalled by the return to high stress reverse faulting conditions below 850-900m depth in the Sydney Basin.

Keywords

In situ stress, coal seam gas, stress anisotropy, stress zone, hydrodynamics, differential stress

1. Introduction

Gas distribution mapping is a key part of coal seam gas reservoir characterisation. In particular, the controlling mechanisms for reservoir development assist with interpretation of exploration and gas production data. On a basin-wide scale coal seam gas distributions can be associated with geological (e.g. Clark and Boyd, 1995; Creech, 1994; Pashin, 1998; Cao et al., 2001; Lamarre, 2003; Draper and Boreham, 2006; Burra and Esterle, 2012), petrological (Bustin, 1997; Faiz et al., 2007a; Scott et al., 2007) and hydrodynamic parameters (Ayers and Kaiser, 1992; Scott, 2002; Lamarre, 2003; Pashin, 2007; Groshong et al., 2009; Pashin et al., 2014). Gas distribution in the Sydney Basin shows a distinct correlation to hydrodynamic and hydrochemical characteristics of groundwater (Burra et al., 2014). The hydrochemical facies evolve from basin margins to the basin centre, and from inland to the coast. Mixed cation bicarbonate-rich fresh waters in recharge areas become increasingly sodium and chlorine-rich along flow paths, towards discharge areas. Meteoric groundwater under hydrostatic pressure penetrates basin sediments until further penetration is restricted by upwelling geopressured basinal fluids and/or reduced porosity and permeability. Gas contents are highest above the nexus between these flow regimes where salinity increases at the base of the hydrostatic-only flow region.

Permeability in coals is mainly related to natural fractures in extensive cleat systems (Gray, 1987; Harpalani and Chen, 1992; Laubach et al., 1998; Groshong et al., 2009). Cleats are thought to form by a number of processes, principally related to coal shrinkage during devolitisation (Pashin et al., 1999; Laubach et al., 1998; Li et al., 2004), expansion during thermal gas generation (Pashin et al., 1999), or in response to tectonic forces post-coalification (e.g. Laubach et al., 1998; Solano – Acosta et al., 2007). Regionally, Kulander and Dean (1993) demonstrated that cleat domains can be related to underlying basement structure and sedimentological geometry, and that the domains can persist though different stratigraphic sequences regardless of lithotypes present. At more local scales, however, cleat intensity and spacing may also be altered in the vicinity of some sedimentary facies, for example, differential compaction effects around sandstone lenses (e.g. Laubach et al., 2000).

In addition to cleats, jointing and fracturing from tectonic processes also have the potential to enhance gas and fluid flow in coals (and other rocks), provided no extensive mineralisation is present (e.g. Laubach et al., 1998). Fracture spacing in rock mass is proportional to the bedding thickness (Ladeira and Price, 1981); and therefore, fracturing in thinly bedded strata is more frequent than in massive competent units such as sandstone lenses or sheets. This has also been observed in coal cleats, where the average cleat spacing was found to be linearly correlated to the thickness of the vitrain bands in the host formation of a given rank (Dawson and Esterle, 2010). In general, dull, high ash and low rank coals have much sparser cleat spacing than bright or high rank coals (Pashin, 2008 and references cited therein) and dull coals in the Sydney Basin were demonstrated to display much higher sensitivity to permeability changes (due to stress) than bright coals (which have higher overall permeability), and this has a significant effect on gas producibility (Bustin, 1997). Coal rank varies spatially across the basin and with depth, as does the present day geothermal gradient.

The effectiveness of these fractures for flow is strongly related to the state of effective horizontal stress (Gray, 1987; Enever et al., 1994a; Jeffrey et al., 1997; Enever and Henning, 1997). This in turn affects coal seam gas producibility (e.g. Ambrose and Ayers, 1991; Sparks et al., 1995). Horizontal stress magnitudes are mainly related to rock properties such as elastic moduli (Enever and Lee, 2000; Dolinar, 2003; Gray, 2011) and these also determine the stress that is borne by different rock types in an interbedded sedimentary sequence (Enever and Lee, 2000; Gray, 2011; Gray et al., 2013).

In situ stresses and coal seam producibility are also known to change around local geological structures, particularly folds and faults, and other features that can limit or enhance fluid and gas flow such as dykes (e.g. Ambrose and Ayers, 1991). Fold structures have been documented to have lower stresses (tension) in the axes, and higher stress magnitudes (compressions) in the flanks of the structures (Teufel et al., 1991; Dawson, 1999; Strout and Tjelta, 2005). Similarly, large faults can affect stress fields both in terms of magnitudes and orientation (Bell, 2006; Kang et al., 2011; Gray et al., 2013), and footwalls of thrust faults have been linked to incidents of gas outbursts in underground coal mines (Cao et al., 2001), which are strongly correlated with large pressure gradient changes (and subsequent alteration of coal properties) induced by mining activities (Cao et al., 2001; Kang et al., 2011; An et al., 2013). Nevertheless, the underlying regional tectonic conditions remain (e.g. Bell, 2006), and it is the basin-wide scale trends that are the interest in the current study.

In general, Eastern Australia, including the Sydney Basin, is under a compressional tectonic regime (Veevers, 2000; Hillis and Reynolds, 2003; Zhao and Muller, 2001; Muller et al., 2012), but stress zonations with depth have been observed in some areas (Enever and Clark, 1997; Brooke-Barnett et al., 2012). The layered characteristic of coal seam gas distributions in the Sydney Basin is hypothesised to be related to these compartmentalised stress regimes. The apparent depth boundaries of the various gas layers coincide with changes in the relative stress magnitudes. This paper maps the relationship between these parameters in the Sydney Basin.

2. Background

The Sydney Basin is a Permo-Triassic coal-bearing sedimentary basin located along the eastern seaboard of Australia (Figure 1). It is a south-easterly trending, asymmetric trough that is narrow in the north and inland areas, and widens as it extends offshore in the east. Inland, the basin margins are defined by a series of monoclines that are present downdip of regional highlands (Figure 1). This geometry results in the regional bedding dip following the outline of the basin towards central and eastern areas, with strata dipping towards the centre of the basin and out to sea in the east (Figure 1). Permian sedimentary strata were deposited during a foreland loading episode of an emerging orogeny, consisting of cycles of marine and terrestrial sedimentation, including coal bearing fluvial to subtidal sequences. Regional syn-depositional and post-depositional folding of strata resulted in coal-bearing sequences lining the basin margin at or near surface, with the same coal seam located down to 1000m depth in the central basin areas. Uplift and subsequent erosion of the youngest coal measures in the more active north-east area in the vicinity of the Hunter-Mookai Thrust Belt (Figure 1) resulted in the outcropping of older sediments in the fault region. As a result, no coal seam is continuously present across the Sydney basin, precluding gas or stress distribution maps on individual horizons. Nevertheless, this setting provided the geometry for the subsequent meteoric influx from inland basin margin locations towards the coastal areas that is associated with the secondary (biogenic and inorganic) generation of coal seam gas distributions in the basin (Burra et al., 2014).

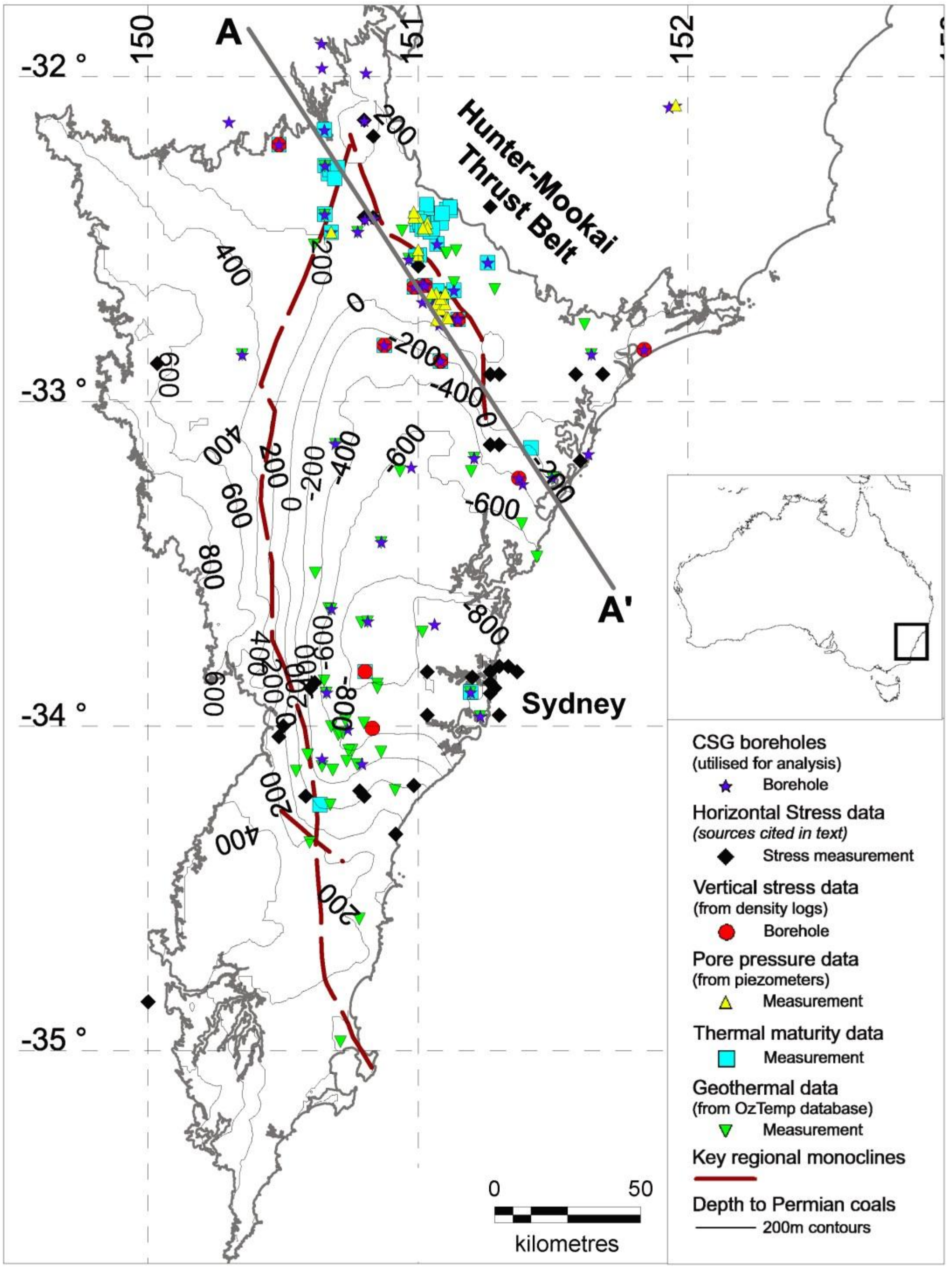

Figure 1. Location map of the Sydney Basin (outline), including location of data points used in this study and the section line shown in Figure 3 and Figure 4.

Coal seam gas distribution in the basin is well-documented, with accumulations dominated by methane, both of biogenic and thermogenic origins, and accessory carbon dioxide, which can form significant volumes in some regions (e.g. Faiz and Hendry, 2006; Pinetown et al., 2008; Thomson et al., 2008). Gas contents range from 0 to over 25m^3/t (raw basis), with shallow horizons under 200 - 300m depth typically less than 5 m^3/t; and middle horizons of 300 - 600m ranging from 8 - 15 m^3/t.

Gas contents in deeper reservoirs show high variance, from single digits to over 25 m^3/t (Burra et al., 2014). This zone of higher gas contents typically persists to approximately 600 - 1000m depth, below which gas concentrations decline or stay constant to the base of the coal measures.

Regionally, the central, eastern and southern areas are dominated by methane-rich reservoirs, whereas the northern inland areas also contain significant CO_2 at depth. CO_2 accumulations mapped in underground coal mines in the southern (Illawarra) region (e.g. Faiz et al., 2003; Faiz et al., 2007b) are considered to be local features, principally limited to the uppermost coal seams (Faiz et al., 2007b) and in gentle anticlinal structures (Faiz at al., 2003). In contrast, CO_2-rich reservoirs in the northern and central regions encompass over 20 major coal seams (comprising over 50 correlatable coal plies and a total coal-bearing strata thickness of up to 300m) and tens of square kilometres in spatial extent (Burra et al., 2014). The source of the CO_2 in these regions have long been considered to be of magmatic origins (Smith et al., 1982; Faiz and Hendry, 2006); however, based on isotopic evidence, other sources such as coal oxidation, biogenic methanogenesis, thermal decarboxylation and dissolution of carbonates cannot be discounted (Smith et al., 1982; Burra et al., 2014). Other gases found in smaller amounts in the basin include wet hydrocarbons and nitrogen. The nitrogen is chiefly associated with near-surface zones around inland recharge areas, indicative of acetate fermentation process; but it also occurs at depth, below the deep CO_2 and ethane accumulations (Burra et al., 2014).

Thermal maturity (i.e. rank) of coals increases with increasing temperature and pressure during coalification (Hunt, 1979; Levine, 1993). Thermogenic gas generation as part of this process was described by Hunt (1979) and is summarised in Figure 2 (Pashin, 2008). The pattern of gas compositional zonation in the Sydney Basin is very similar to this sequence; however, the rank ranges differ substantially. Additionally, the gas zone boundaries are diffuse, cross-cut specific coal sequences and structure (Thomson et al., 2008; Burra et al., 2014), and the gas, particularly in shallow areas, have been shown to be isotopically of biogenic origin (Smith et al. 1992; Faiz et al., 2003).

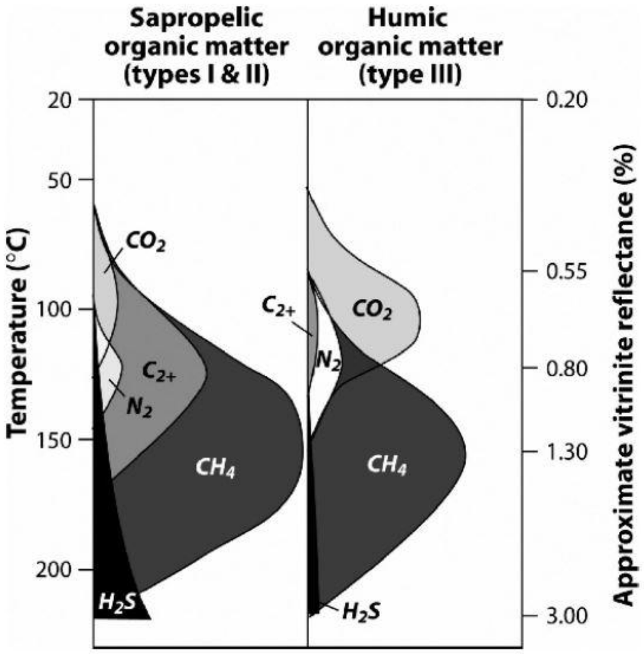

Figure 2. Thermogenic coal seam gases generated during coalification with varying temperature and thermal maturation, described by Hunt (1979) (Pashin, 2008).

The extent of biogenic gases in the subsurface is considered to be controlled in large part by the infiltration patterns of meteoric waters (Smith et al., 1992; Scott et al., 1994; Pashin, 2007) and their chemical composition (Burra et al., 2014).

In the Sydney Basin, strata down to ~800 - 1000 m depth host both fresh and brackish groundwater under hydrostatic flow according to the local hydrostatic pressure gradient; at greater depths, upward-moving saline waters are mobilised in response to geopressured conditions (Figure 3). Hydrostatic meteoric water influx introduces methanogenic consortia into the system (e.g. Scott et al., 1994; Scott, 2002) that produce shallow biogenic methane gas accumulations. Gas contents typically peak at this horizon below which gas volumes decrease (Figure 4) (Burra et al., 2014). In the biogenic zone, calcium-rich fresh waters in the highland recharge areas cause the dissolution of carbonates present in fractures and cleats (Staub, 1995a; Golab, 2003), which results in the enrichment of bicarbonate in groundwaters (Back et al., 1993). The bicarbonate-rich waters predominantly move down-gradient along the flow path; however, some volumes are partially dispersed to deeper layers via sub-vertical fractures associated with basin-margin monoclines and other geological structures (Burra et al., 2014). This dispersion can result in the formation of a ‘deep’ CO_2-rich gas layer between the biogenic and thermogenic methane layers that are associated with the hydrostatic and geopressured flow regimes, respectively. With increasing sodium concentrations in the groundwater (down-gradient and with depth), excess bicarbonate precipitates as calcite along fractures and coal cleats (Runnells, 1993). This later stage development has occurred in the central parts of the Sydney Basin, where secondary calcite infill has been observed to post-date earlier carbonate mineralisation in fractures and cleats (e.g. Staub, 1995b).

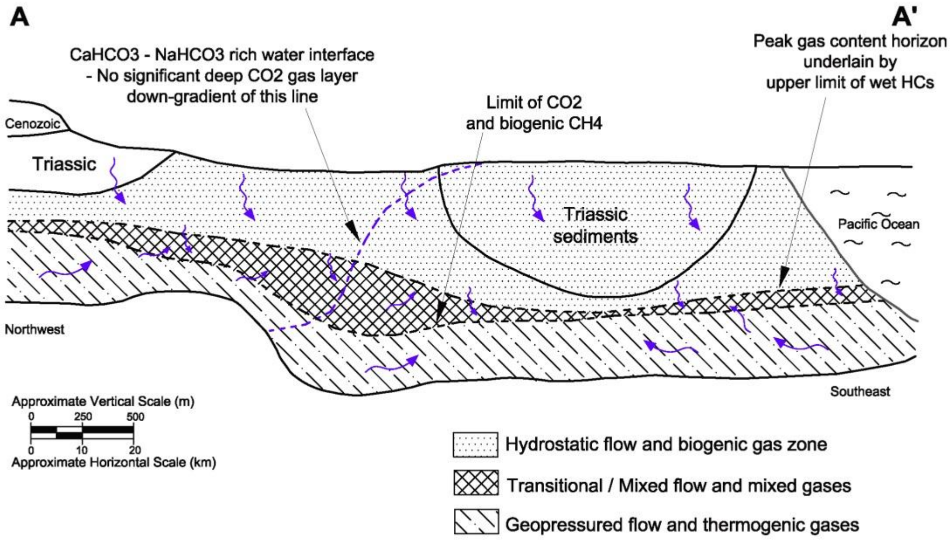

Figure 3. Conceptual model proposed for Sydney Basin hydrodynamic flow regime and gas compositional zonation (after Burra et al., 2014).

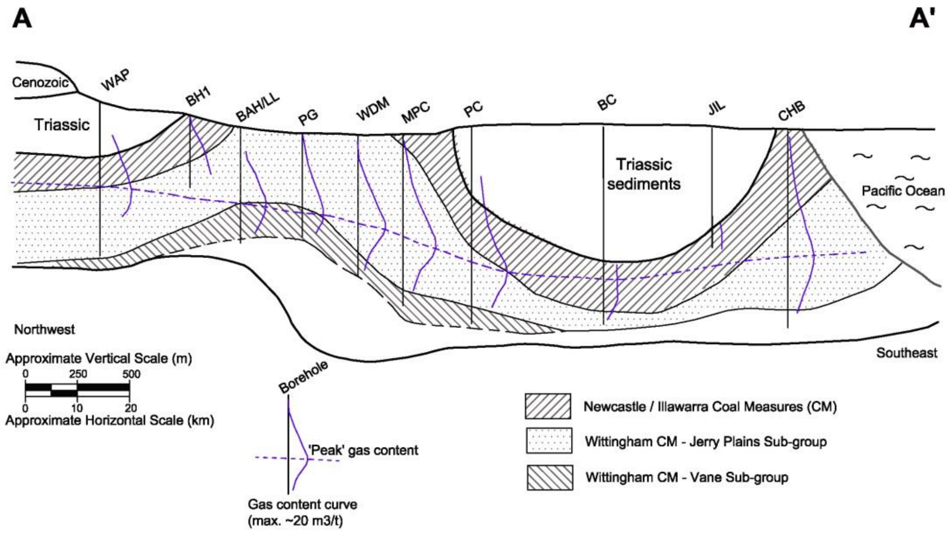

Figure 4. Schematic cross section of typical gas content trends across the Sydney Basin. 'Peak' gas content horizon is indicated by the dashed line. Location of section line is shown in Figure 1. (For more detail on the underlying borehole data, refer to Burra et al., 2014).

Groundwater flow is facilitated by permeability. Permeability in coals has been reported to be closely related to effective horizontal stress magnitude (e.g. Gray, 1987; Enever, 1994a), and this requires an assessment of *in situ* stress regimes. Effective stress is the total stress acting on the rock mass minus the pore pressure exerted by pore fluids (Zang and Stephansson, 2010; Zoback, 2010). Three principal stresses act on the rock mass, and these are generally modelled as one vertical (Sv) and two horizontal (maximum (SH) and minimum (Sh)) stresses (Zang and Stephansson, 2010; Zoback, 2010). Vertical stress is derived by assuming that it originates from the weight of the overburden strata, and it is calculated from the density (ρ) and thickness (h) of the overlying rock mass and the gravity term (g):

$$\mathrm{Sv} = \rho\mathrm{hg} \qquad \text{Eq.1}$$

To derive horizontal stress magnitudes, models generally assume that rocks behave elastically, and depending on the level of detail, a uniaxial or a biaxial approach is taken (Katahara, 1996; Zang and Stephansson, 2010; Zoback, 2010). The uniaxial approach assumes that (equal) horizontal stresses are generated by the vertical stress and the elastic properties of the overlying rocks.

$$\mathrm{S(H\ or\ h)} = \frac{v}{1-v}\mathrm{Sv} \qquad \text{Eq. 2}$$

where ν is the Poisson's ratio.

In the biaxial model, the uniaxial method is expanded to include a tectonic strain term, representing far-field tectonic forces. Thus, Eq. 1 is expanded

$$\mathrm{SH} = \frac{v}{1-v}\mathrm{Sv} + \frac{E}{1-v^2}(v\varepsilon\mathrm{h} + \varepsilon\mathrm{H}) \qquad \text{Eq. 3}$$

$$\mathrm{Sh} = \frac{v}{1-v}\mathrm{Sv} + \frac{E}{1-v^2}(v\varepsilon\mathrm{H} + \varepsilon\mathrm{h}) \qquad \text{Eq. 4}$$

where E is the Young's modulus, and ε is the tectonic strain in the minimum and maximum horizontal stress directions.

The relative magnitudes of the three principal stresses determine the dominant tectonic regime affecting the rock mass. The Anderson fault classification describes the characteristics of the three main stress regimes (Zang and Stephansson, 2010; Zoback, 2010; Meng et al., 2011; Flottman et al., 2013):

- normal: Sv > SH > Sh
- strike – slip: SH > Sv > Sh
- thrust or reverse: SH > Sh > Sv

Generally, an overall tectonic regime dominates a region as a whole, but parts of the subsurface may experience contrasting forces acting on them where stress discontinuities (Stephansson, 1993) develop as stress is redistributed in some areas but not others (Bell, 1996). These differences are mainly controlled by rock strength (e.g. elastic moduli) (Enever et al., 2000; Dolinar, 2003; Zoback, 2010), and are also considered in terms of stress anisotropy, with low stress anisotropy referring to two principal stresses becoming similar in magnitude (upon stress transfer from a more dominant to a less dominant stress component) (Bell, 1996; Enever et al., 2000; Yale, 2003). For example, stress fields in the Bowen and Surat Basins of QLD, Australia, exhibit a reverse tectonic regime in strata down to 400m depth, below which strike-slip conditions prevail (Brooke-Barnett et al., 2012; Flottman et al., 2013). In some boreholes, a further stress zone is apparent below 900m depth. This vertical zonation in the different areas significantly impact on the direction and style of hydraulic fracture propagation (Flottman et al., 2013).

Understanding the *in situ* stress environment is an important aspect of reservoir characterisation, particularly with regards to gas generation (secondary, biogenic), migration and/or entrapment in a sedimentary basin. *In situ* stress may ultimately determine the observed gas distributions locally and regionally in some basins, and it may be possible to utilise this understanding to use geological mapping for the purposes of forecasting likely gas accumulations in coal-bearing sedimentary basins.

2.1 Objectives

The aim of this paper is to consider mechanisms that can produce the observed vertical coal seam gas zonation in the Sydney Basin. This zonation has been shown to be strongly related to the regional hydrogeological regime (Burra et al., 2014) which has the potential to produce the 'cross-cutting' nature of the gas zones in relation to reservoir geometry. In consideration of the naturally fractured character of coal seams as the primary migration path for fluid and gas permeability in coal reservoirs, the influence of *in situ* stress acting on this system is the most likely control of this system. As a result, the analysis reported in this paper concentrates on establishing the characteristics of the *in situ* stress field present in the basin, with particular focus on the interplay between the different stress component magnitudes and the identification of stress and other discontinuities present in the sequence that may result in the gas zonation over-printing the host strata geometry.

3. Methodology

3.1 Data

In situ stress and coal seam gas data were compiled from publically available information from the New South Wales (NSW) Department of Trade and Investment's Digital Imaging Geological Systems (DIGS - http://digsopen.minerals.nsw.gov.au/) and Minview (http://minview.minerals.nsw.gov.au/mv2web/mv2) databases, and published articles. Pore pressure data were sourced from regional observation wells (piezometers) provided by a coal mining company with coal mines located in the northern part of the Sydney Basin, as well as from DIGS (3 boreholes). The private borehole measurements originated from vibrating wire piezometers after these units had been calibrated to the *in situ* conditions (1-2 months after installation but a number of months prior to the start of pressure draw-down); the public borehole data points were reported from regional pressure testing and were used as reported by the original programs. There are 130 pore pressure sample points from 20 wells, ranging from 16m to 483m, with the borehole locations shown in Figure 1. Six additional data points from a single borehole in the nearby Gloucester Basin are also used qualitatively to provide a control on the approximate lower extent of the pressure gradient between 814m and 1106m depths.

Coal seam gas data consist of 23 boreholes and 1164 samples, and includes gas content (on an 'as received' or 'raw' basis) and composition (476 samples; reported on air-free basis), as well as information about the coal samples such as depth, ash and moisture contents, and host stratigraphic formation. Gas data are mainly used for the analysis of gas trends against depth and to probe relationships with *in situ* stress characteristics. Gas data are analysed 'as received' to compare to *in situ* conditions.

Coal rank data are similarly collated from DIGS borehole data and are principally used to establish the nature of the thermal maturity in the basin - particularly against depth, because the spatial distribution of coal rank in the basin has previously been reported to increase towards the southern part of the basin (Faiz et al., 2003; Scott and Hamilton, 2006; Pinetown, 2014). A total of 435 sample points originating from 44 boreholes are utilised; with 145 samples originating from the DIGS database and complimented by a further 270 samples from a private mining dataset limited to under 400m depth.

Temperature data were sourced from the OzTemp well temperature database from the Geoscience Australia website (Holgate and Gerner, 2010), and these had been collated from regional stratigraphic and petroleum drilling programs. 303 data points from 59 boreholes are located in the Sydney Basin and are used for establishing the geothermal gradient(s) and to validate the limit of meteoric influx into the basin. The location of the boreholes is shown in Figure 1.

In situ horizontal stress magnitude data were collated for the analysis, the location of boreholes is shown in Figure 1. Only field measurement data obtained by hydraulic fracturing and over-coring are utilised, which have been shown to produce consistent results (Gale et al., 1984b; Enever, 1993). Vertical stress was derived using conventional wireline log (long spaced density) interpretation methods (described in the next section). Wireline density logs were obtained from DIGS and their locations are shown in Figure 1.

3.2 *In situ* stress calculation and analysis

The vertical stress (Sv) gradient was derived from to the long-spaced wireline density logs using Eq.1 (Fertl, 1976; Zang and Stephansson, 2010; Zoback, 2010), where the gravitational constant is 9.8 m/s^2. Horizontal stresses can be calculated in a number of ways, as detailed previously; however, direct measurement is always more desirable for accuracy. *In situ* stresses are normally determined from interpreting logs obtained from either over-coring or hydraulic fracturing tests. The particulars of the field tests and their interpretation are detailed elsewhere (Evener, 1993; Hillis et al., 1999; Peng, 2007; Zang and Stephansson, 2010). For the current study, consistency in interpretation of the field test results was sought, and for this reason, the horizontal stress dataset used in analysis was collated from literature using these field tests methods. Data were compiled from Enever et al. (1994a, 1994b), Enever et al. (1998), Hillis et al. (1999), and Enever and Lee (2000). To calculate effective stresses in the basin, Terzaghi's effective stress equation is utilised by subtracting the pore pressure from the total stress magnitudes for three principal stress components (Zoback, 2010). Normally, pore pressure is estimated using the vertical stress equation (Eq. 1) and assuming a density for fresh water of 1.0 g/cm^3 (i.e. a pressure gradient of 0.45 psi/ft; Dake, 1978). However, actual pore pressure data from piezometers in Sydney Basin regional observation wells allow a more accurate estimation of the pressure gradient, and two linear equations were obtained for use in the effective stress calculations (see Section 4.2 in Results). Unfortunately, no 'total dissolved solids (TDS)' data is available to ascertain the linearity of this trend; however, resistivity logs indicate such conditions prevailing in various parts of the basin.

To investigate the *in situ* stress characteristics fully, stress anisotropy is determined from the difference between the two horizontal stress magnitudes. Uniform major and minor horizontal stress magnitudes are indicative of stress transfer having occurred between strata layers via shearing and a disparity implies that such transfers have not transpired (Enever et al., 2000; Yale, 2003; Bell, 2006; Flottman et al., 2013). Stress compartmentalisation and overall characteristics are also assessed using the Anderson faulting classification (Zang and Stephansson, 2010; Zoback, 2010; Brooke-Barnett et al., 2012; Flottman et al., 2013).

4. Results

4.1 Coal and coal seam gas

Coals in the Sydney Basin are principally bituminous with vitrinite reflectance ranging from 0.6% to 1.7% Romax (Figure 5), with reports of up to 2% (Middleton and Schmidt, 1982; Bocking and Weber 1993). In general, thermal maturity increases with depth, and spatially, it increases towards the southern part of the basin (Scott and Hamilton, 2006) but this is partially due to the fact that the coals seams are located at greater depths in that region.

There appears to be a marked change in the rank gradient at approximately 850m depth which coincides with changes in other key parameters discussed in this paper. A less prominent inflection point occurs at around 400m, below which rank 'stabilises' at an average of 0.8% down to the 850m horizon (Figure 5). The cause of the changes in the rank gradient is unknown but may be indicative of different stages of burial and/or heat flow in the basin evolution.

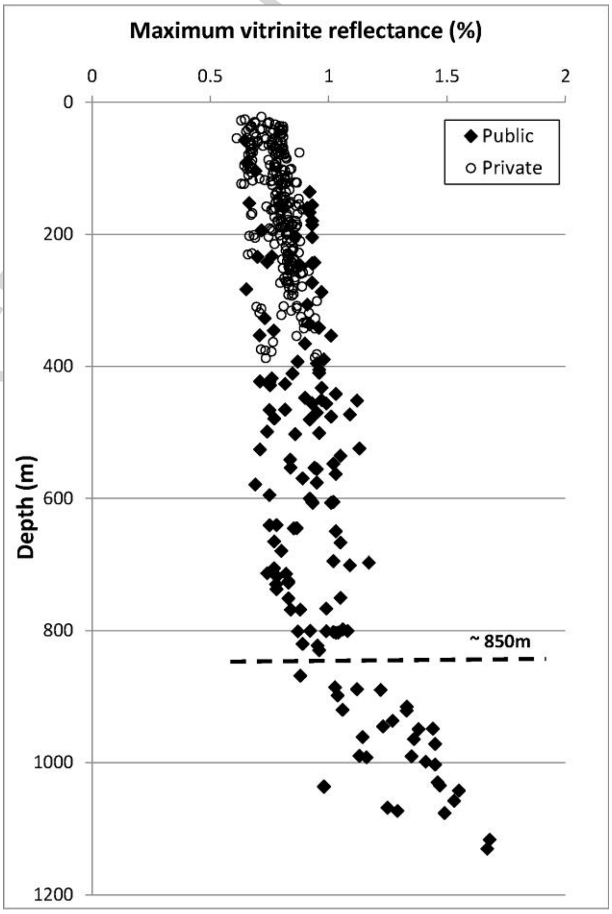

Figure 5. Maximum vitrinite reflection with depth in the Sydney Basin. Labels indicate data source.

A similar pattern is apparent in the geothermal gradient in the basin. The overall, geothermal gradient of the Sydney Basin is approximately 25°C/km which is similar to other basins on the east coast of Australia (e.g. 23°C/km in the Clarence – Moreton Basin – Haynes, 2012) but higher than some basins in the USA (e.g. 16.9°C/km in the Black Warrior Basin – Pashin and McIntyre, 2003). The main heat sources in the Sydney basin are thought to be the presence of volcanics and granites in the basement and the thickness of the sedimentary strata (Facer et al., 1980, Middleton and Schmidt, 1982). The presence of thick coal sequences may also be a factor as these units have an insulating effect on the surrounding strata and can contribute to higher than normal heat flows, as demonstrated by Cercone et al. (1996) in the Appalachian Basin in Pennsylvania, USA. In the Sydney Basin, the geothermal gradient shows a marked change between 800 - 1200m, with the depth of the inflection point increasing towards the southern part of the basin (Figure 6). This depth range is compatible with published porosity and permeability data (Blevin et al., 2007) which shows both parameters decreasing to and then levelling out below 800 - 1200m. This horizon is interpreted to represent the extent of meteoric influx in to the basin (Burra et al., 2014), also evidenced by the concave shape of the geothermal curves above the inflection points in Figure 6 which represent recharge conditions (Anderson, 2005). Carbon isotope data presented in Burra et al. (2014) further supports this conclusion.

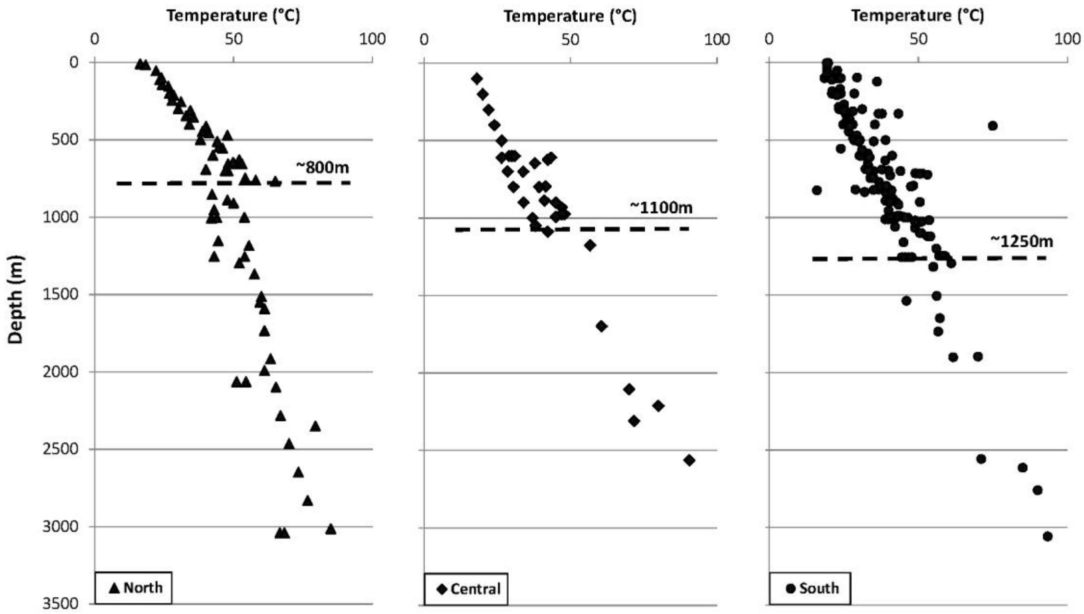

Figure 6. Temperature with depth in the Sydney Basin (Source: OzTemp database, Geoscience Australia https://data.gov.au/dataset/oztemp-well-temperature-data). Dashed lines indicate depth of change in geothermal gradient in the 3 main parts of the basin.

Coal seam gas contents in the basin range from 0.1 - 27.4 m^3/t, increasing with depth to a 'peak gas' horizon around 600 - 900m depth, below which contents generally decrease, forming an apparent parabolic trend (Figure 7 Part A). This trend is evident in both 'as received' (or raw) and dry-ash free corrected data. In this study, 'as received' information is used to be directly comparable to *in situ* stress states. Gas composition is varied and is comprised of a number of important gas types: CH_4

and CO_2, as well as minor wet gases and N_2. Methane, carbon dioxide and nitrogen compositions can range from zero to near 100%, whereas ethane does not exceed ~10%.

Biogenic methane is found at less than ~800 - 1000m depth, and thermogenic methane is concentrated in deep coal seams (Faiz et al., 2003; Burra et al., 2014). In the inland (western, central and northern) areas, CO_2 is present between these two principal intervals, but does not occur in the eastern and much of the southern part of the basin, although locally there are coal mines with high CO_2 levels at shallower depths (Faiz, 2007b). Ethane is associated with the top of the thermogenic gas zone and occurs at the interface of the two methane layers, or overlaps with part of the CO_2-rich layer (where it is present). The overall peak gas content trends with depth for all three gas types show the same gradually deepening pattern towards the central and southern areas (Figure 7). Notably, gas contents are commonly higher in the northern and central areas, where coal rank is lower and 'peak gas' is located at shallower horizons than in the central and southern areas (Figure 7). In general, the gas content peak occurs between 500 - 1000m depth and is encountered deeper in the more open coastal regions in the east and south (Figure 7).

The CO_2 peaks are driven by the relative proportion of this gas in the different regions, with the northern areas hosting significant CO_2 volumes and concentrations decreasing towards the central and southern areas. In areas where the deep CO_2 layer exists, the peak CO_2 content occurs below the corresponding CH_4 and total gas content peaks. The central area exhibits a noticeable reduction in CO_2 concentration in the deep CO_2-rich layer, located in the western part of that area, and there is no deep CO_2 present in the northern and eastern parts of the central Sydney Basin. The significance of this is that the total gas (and CH_4) trends for the central area in Figure 7 show two peaks, one around 550m depth, originating from the western part of the area, and another at 850m. The latter anomalous peak originates from a single borehole in the northern part of the area in the vicinity of a large fault. In light of this, the peak in CH_4 gas occurs above the peak in CO_2 in this area, in line with the other areas of the basin.

Ethane data are limited both by volume of gas present in the basin (i.e. it is a minor gas, comprising generally less than 5% of total gas composition in affected samples) and by final depths of boreholes in the region. Ethane only occurs at depths greater than 500 - 1000m, and total depths of a number of boreholes do not reach these horizons. Table 1 shows the numbers of boreholes and samples used in producing the trends shown in Figure 7.

Gas saturation in the basin is complex due to the presence of a number of different gas types. Sorption capacity of coals varies with gas type, pressure, temperature and coal properties reflecting rank, and is commonly determined by experimental measurement under changing pressure conditions at a given temperature. The resultant isotherm indicates the maximum gas holding capacity of the sample and is then used to calculate the gas saturation based on the measured gas content of the sample. In the case of mixed gas samples, a mixed gas isotherm must be calculated and this varies significantly between a sample with 100% CH_4 or CO_2 concentrations – both common conditions in the Sydney Basin. Consequently, gas saturation can range from near 100% saturation to under 30% saturation when high CO_2 concentrations or mixed gases are present. Therefore, gas saturation can only be determined on sample specific basis and this precludes the regional assessment of gas saturation with depth or basin area.

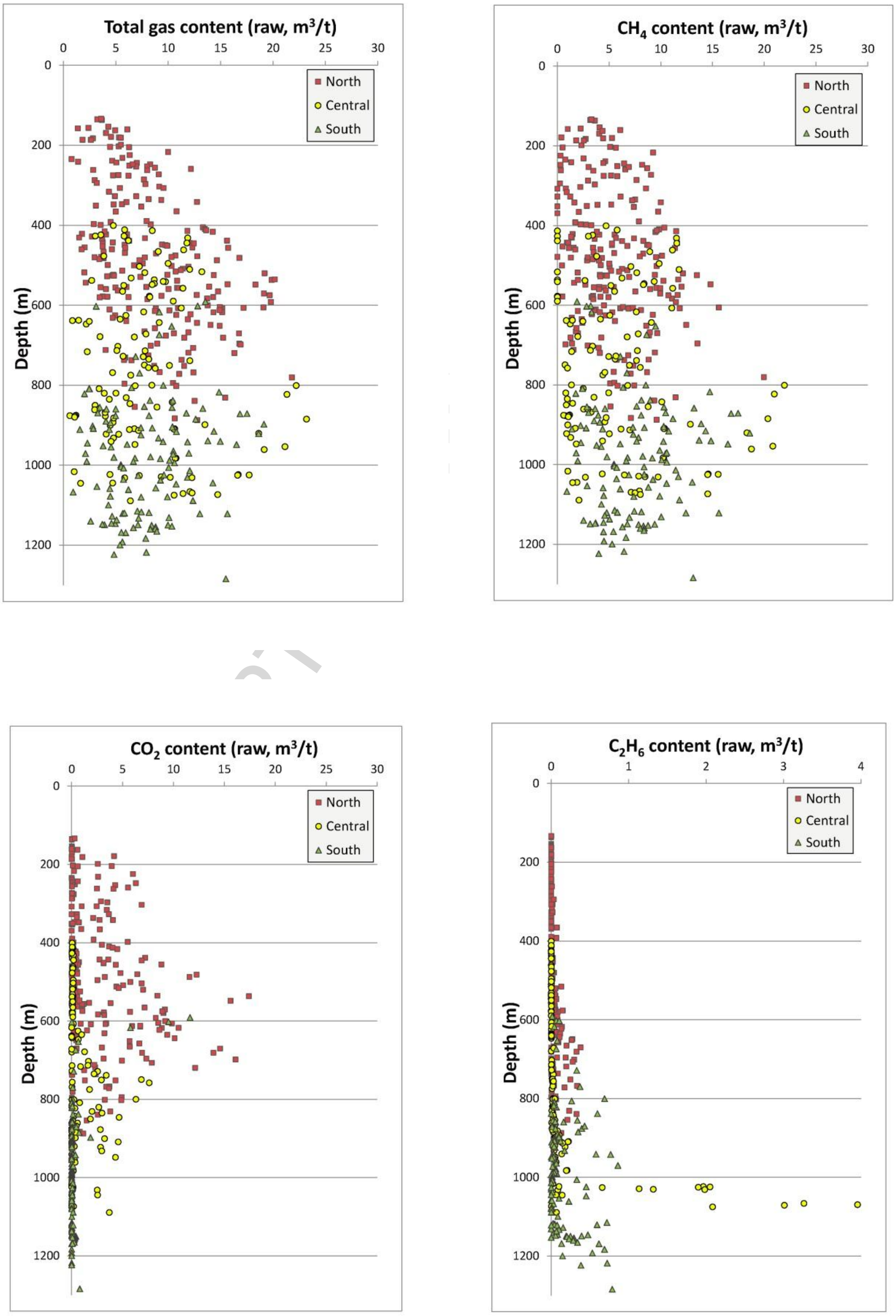
Total gas content (raw, m³/t)
CH4 content (raw, m³/t)
CO2 content (raw, m³/t)
C2H6 content (raw, m³/t)
Depth (m)
North
Central
South
0
5
10
15
20
25
30
1
2
3
4
200
400
600
800
1000
1200

Figure 7. Gas content and composition trends with depth in the Sydney Basin. Part A (top left): total gas content (m^3/t); Part B (top right): methane content (m^3/t); Part C (bottom left): carbon dioxide content (m^3/t); Part D (bottom right): ethane content (m^3/t) - Note change of horizontal scale in Part D.

Region	Number of boreholes	Number of samples
North	15	604
Central	8	297
South	9	235

Table 1. Number of gas samples used in gas trends shown in Figure 7.

Gas content has an intriguing relationship with coal thermal maturity in the Sydney Basin. At a simplistic level, there appears to be no close relationship between the two variables, as coal rank continues to increase below depths where gas contents decrease from the 'peak gas' horizon (Figure 5 and Figure 7). However, when these parameters are plotted directly against each other (Figure 8), a striking pattern emerges that resembles the trends predicted by the Hunt diagram (Figure 2) which was developed from experimental thermogenic gas generation from coals. This is unexpected because the rank ranges of coals in the Sydney Basin are higher than those indicated on the Hunt diagram for some of the gas types and much of the coal seam gases at shallower than 800m depth in the basin are of biogenic and inorganic origins (e.g. Burra et al., 2014). According to the data, at any given rank, a wide range of gas contents can be present in place (cf. Pashin, 2010), and this is also the case for the gas composition trend with depth. In this manner, the thermal maturity may define the upper limit of possible gas contents (e.g. sorption capacity), but some other phenomenon controls the levels of gas saturation (discussed in Section 5). In other words, "the isotherm is not the law, it is the limit" (J. Pashin, pers. comm.).

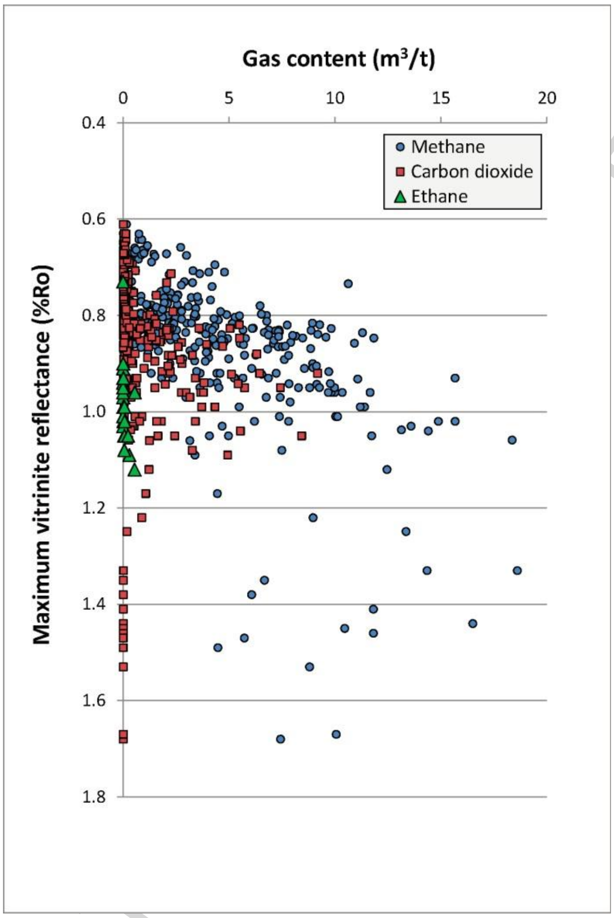

Figure 8. Maximum vitrinite reflectance against gas content of various gas types in the Sydney Basin.

4.2 Pore pressure

Pore pressure data from vibrating wire piezometers from regional observation wells are available to a depth of 483m (Figure 9). Pressures range from 0.05 MPa at 20m to 5.08 MPa at 463m. Most of the pore pressure data used in the analysis were recorded from approximately two months after the installation of the various piezometers (to allow the equipment to calibrate to *in situ* conditions), and at least six months prior to any gas drainage in the local areas. The remainder (6 data points) was obtained from publically available well-testing of regional boreholes to supplement the mine-site dataset. The recorders monitor various coal seams, with up to 8 units (i.e. 8 coal seams) in a single well. The data shows a generally consistent hydrostatic pressure gradient with depth, indicating a water table of around 40m depth. This is consistent with observations from exploration boreholes in the region (e.g. Thomson et al., 2014); however, a change in the pressure gradient is apparent at approximately 320m depth (Figure 9). The cause of this change is unknown; however, it is not associated with any particular stratigraphic horizons or coal properties.

Regression formulas were fitted to these two populations, and the results used to derive effective stress magnitudes. Whereas pore pressure measurements were not available for depths below ~500m in the Sydney Basin, sparse pore pressure readings from the nearby Gloucester Basin from 814 - 1106m depth support the approximation of pressures at these depths (ranging from 7.9 to 12.5

MPa). Additionally, regional porosity data from the Sydney Basin shows that much of the basin is under hydrostatic pressure down to approximately 800 - 1000m depth (Blevin et al., 2007; Burra et al., 2014). It is possible, however, for local overpressure to occur in boreholes, particularly near major structures, as evidenced by a number of artesian wells drilled in the northern part of the basin.

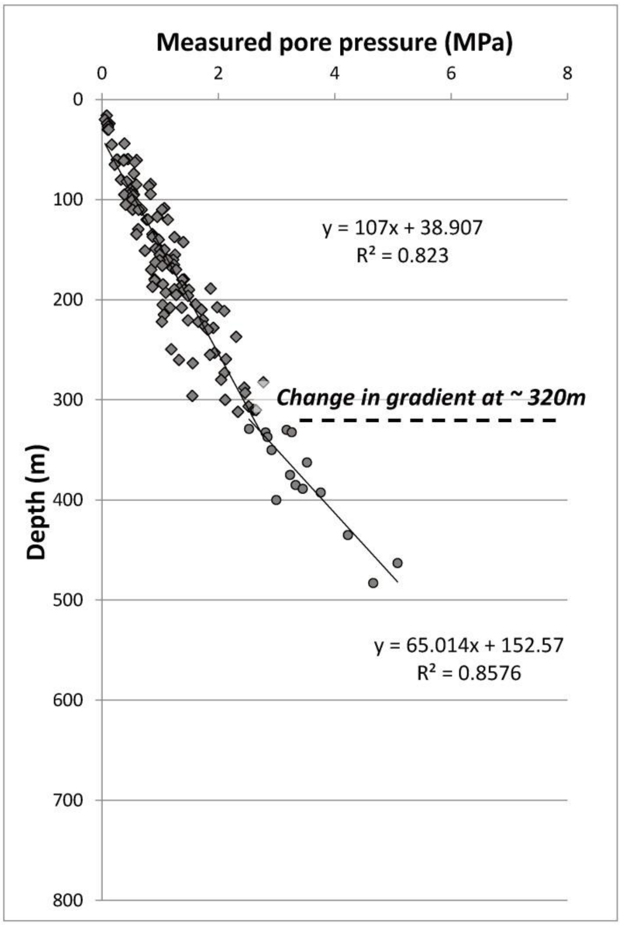

Figure 9. Pore pressure measurements from piezometers in the Sydney basin plotted against depth.

4.3 *In situ* stress magnitudes

Vertical stress estimated from overburden density using ten regionally representative boreholes show lithostatic gradients ranging from 22.5 MPa/km to 26.5 MPa/km, or a 2.3 to 2.7 g/cm^3 overburden density (Figure 10). This is in agreement with previous estimates ranging from 2.3 g/cm^3 (Hillis et al., 1999) to 2.5 g/cm^3 (Enever, 1993; Enever and Clark, 1997; Enever et al., 2000). For the current study, a gradient of 24.5 MPa/km, or 2.5 g/cm^3 density, is adopted to represent the vertical stress in the basin.

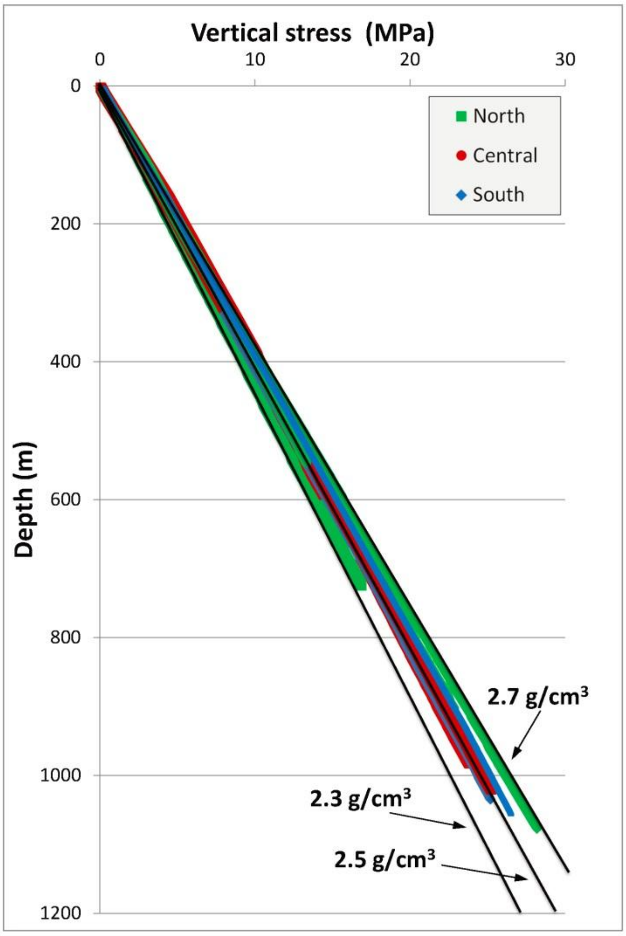

Figure 10. Vertical stress gradients derived from wireline density logs from 10 regional boreholes shown in Figure 1.

Horizontal stress magnitudes were collated from the literature (Enever et al., 1994a, 1994b; Enever et al., 1998; Hillis et al., 1999; Enever and Lee, 2000) and are plotted in Figure 11 with the vertical stress and pore pressure gradients. Horizontal stress magnitudes range from ~0.2 to 55 MPa between 0.1 and 980m depth. In general, both minimum and maximum horizontal stress magnitudes increase with depth, but can vary significantly at any interval (Figure 11), particularly in the shallow horizons. In some sections, the stress magnitudes increase in a linear manner (e.g. surface to 200m) and elsewhere, the increases are more compartmentalised, and a number of stress zones are apparent. More specifically, Figure 11 shows that the initial linear increase below surface gives way to widely ranging stress magnitudes between ~ 200 - 400m depths (0 - 53 MPa), which is followed by another zone of still variable but more consistent magnitudes down to 650m (4.0 - 40 MPa). Between 650 - 900m depth, both horizontal components show significantly lower magnitudes but increase again below this horizon to the highest values observed in this dataset.

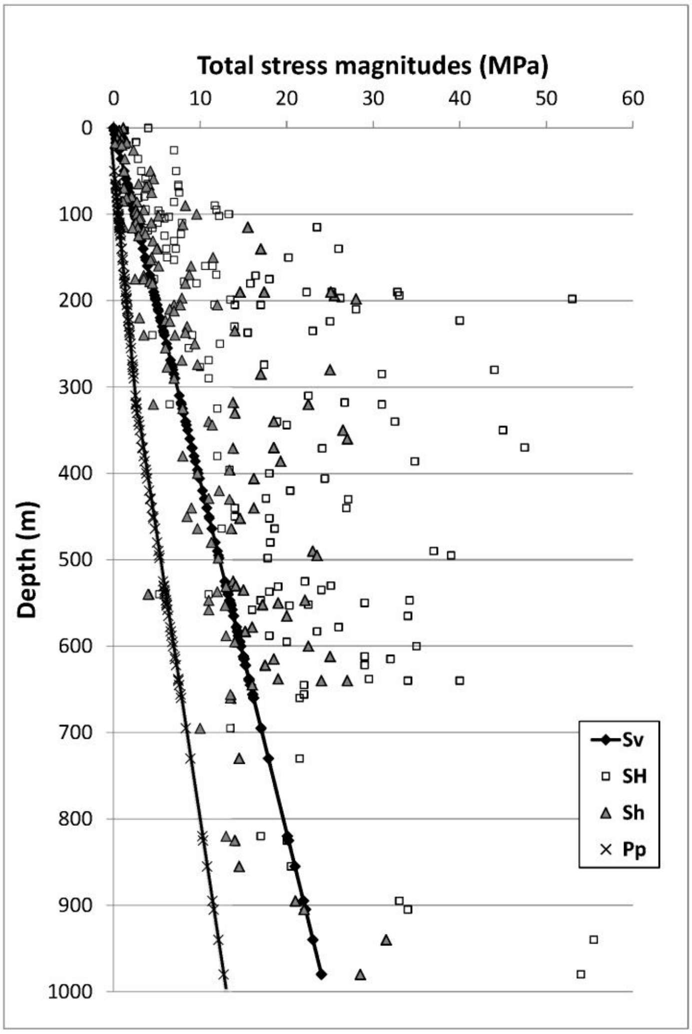

Figure 11. Total stress magnitudes with depth in the Sydney Basin (Horizontal stress data compiled from Enever et al., 1994a,1994b; Enever et al., 1998; Hillis et al., 1999; Enever and Lee, 2000. Vertical stress and pore pressure gradients derived from borehole data; see text for methodology). Sv = Vertical (overburden) stress; SH = Maximum horizontal stress; Sh = Minimum horizontal stress; Pp = Pore pressure.

Total stress magnitudes were transformed into effective stress data by subtracting the pore pressure. The resultant data set is shown in Figure 12. In general, the stress magnitudes are minimally affected at shallower than 400m depth, and horizontal stresses are essentially unchanged throughout the full strata sequence due to their significantly higher total magnitudes than pore pressure in the basin. However, the effective vertical stress gradient below this horizon is noticeably affected and it becomes approximately equal to the pore pressure at ~650m depth.

The pore pressure – effective vertical stress “cross-over” is an unusual situation which could imply, at a simplistic level, the fracturing of the strata under its own weight. However, two observations can be made in relation to this occurrence in the data. This “overlap” of the two trends may be the artefact of using an incomplete dataset that assumes a similar continuing trend with depth as observed at shallower horizons (i.e. pore pressure data is only available down to ~500m depth in this region). Further, the vertical stress is calculated by assuming that only the weight of the overburden strata is acting on rocks at a given depth, and no consideration is given to possible additional stresses originating from the horizontal stress component, particularly in a compressional environment. Nevertheless, the change in pore pressure gradient at 320m depth is real (based on direct measurements (Figure 9)), and the depth at which the apparent Sv – Pp equalisation occurs also coincides with a significant change in the horizontal stress regime including the differential horizontal stress magnitudes (discussed below). Indeed, pore pressure can be greater than the effective vertical stress under some circumstances (e.g. Zhao et al., 1998; Hillis, 2000); however, this phenomenon has not been extensively studied in compressive regimes. In this study, it is observed that it could potentially be related to the marked change in horizontal stress regimes around this depth in the basin; else, it could be indicative of ‘over-pressured’ conditions for example due to hydrocarbon generation (J. Pashin, pers. comm.).

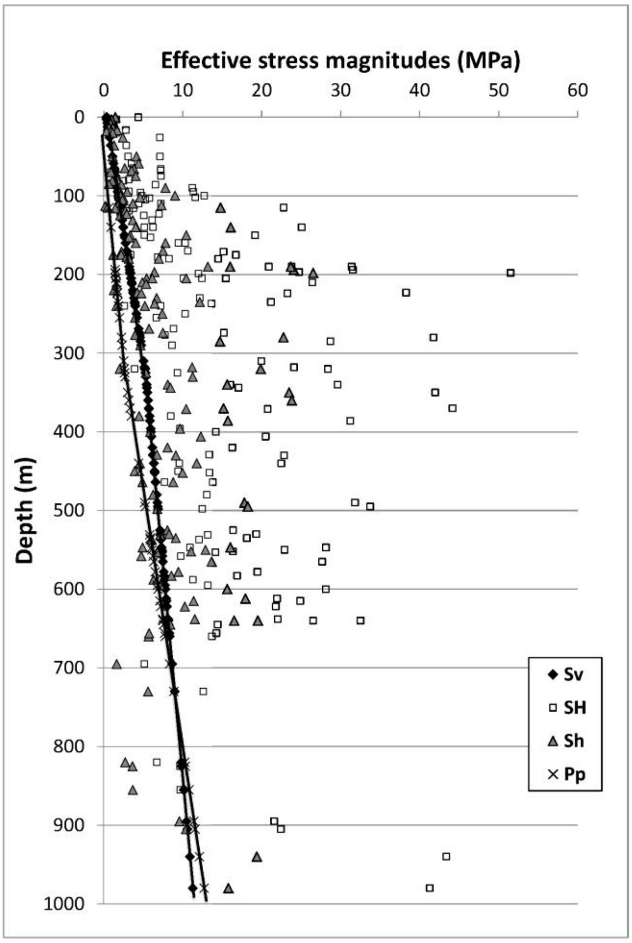

Figure 12. Effective stress (i.e. total stress minus pore pressure) magnitudes with depth in the Sydney Basin (derived from data presented in Figure 11). Sv = Vertical (overburden) stress; SH = Maximum horizontal stress; Sh = Minimum horizontal stress; Pp = Pore pressure.

Horizontal stress magnitude differences indicate stress anisotropy that is related to changing stress conditions (e.g. Gray, 1987; Enever and Clark, 1997). Figure 13 shows the horizontal stress differences derived from the horizontal stress magnitudes in Figure 11. Low differential magnitudes represent strata that has experienced some (or significant) level of stress relief, whilst high values show strata that are unevenly affected in the two different horizontal stress directions (i.e. anisotropic). The overall trend mirrors those observed in Figure 11 and Figure 12; however, the closer clustering of the data within each stress zone suggests more consistent conditions than implied in the stress magnitude plots. It also highlights that the horizontal stress zone changes with depth are sudden and marked, regardless of the absolute stress magnitudes at those horizons. This depiction therefore provides a more consistent and comparable platform to investigate relationships between stress field characteristics and gas distributions.

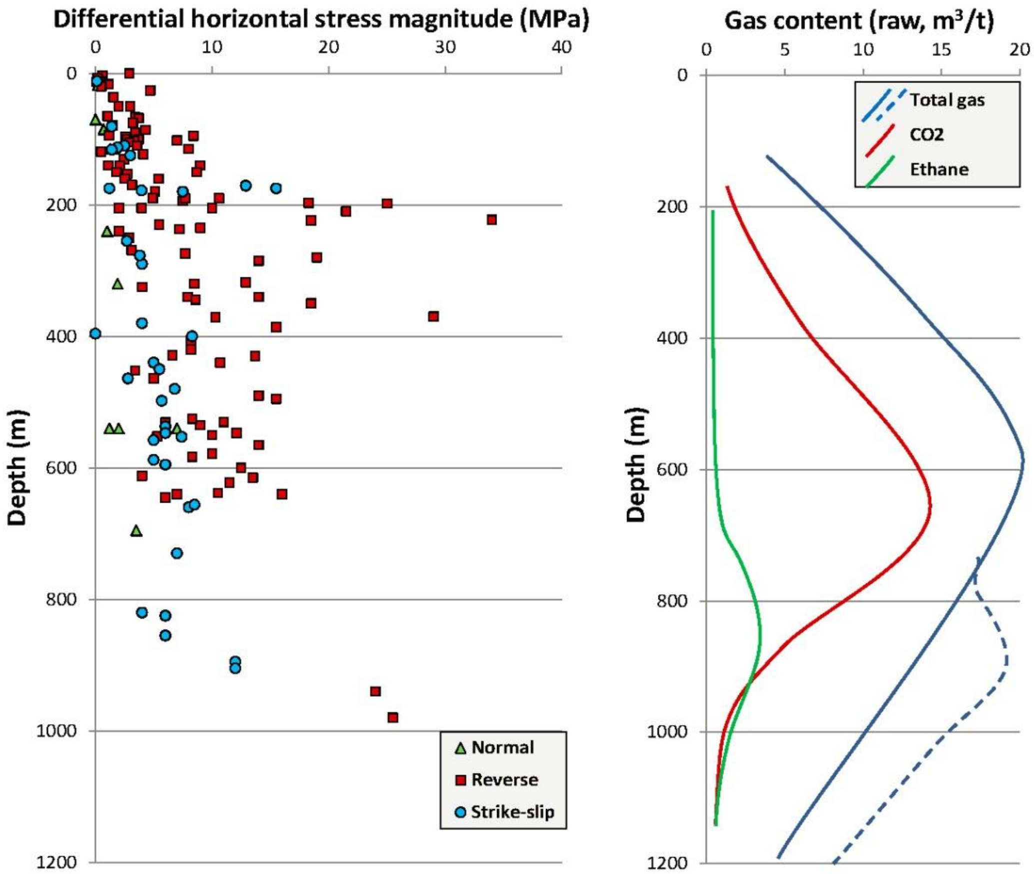

Figure 13. Part A (left): Differential horizontal stress magnitudes with depth in the Sydney Basin (derived from data presented in Figure 11 and colour-coded to depict tectonic regime). Part B (right): generic gas trends in the Sydney basin (derived from data in Figure 7; dashed blue line indicates thermogenic gas peak in limited areas). Trend lines are qualitative.

Another way to represent this phenomenon is to plot the average horizontal stress component normalised by the vertical stress (SHh average / Sv) against depth (Figure 14). This is known as the lateral stress coefficient, K, (Brown and Hoek, 1978; Teufel et al., 1991; Bjorlykke and Hoeg, 1997; Zang and Stephansson, 2010; Meng et al., 2011) and has been presented in modified versions by various authors (e.g. Kang et al., 2010; Mark and Gadde, 2010; Liu, 2011) to plot SH/Sv and Sh/Sv separately (total or effective stresses), with similar results. This coefficient is plotted in tandem with the differential horizontal stress to reiterate the marked changes between different zones in the horizontal stress profile in the vertical plane.

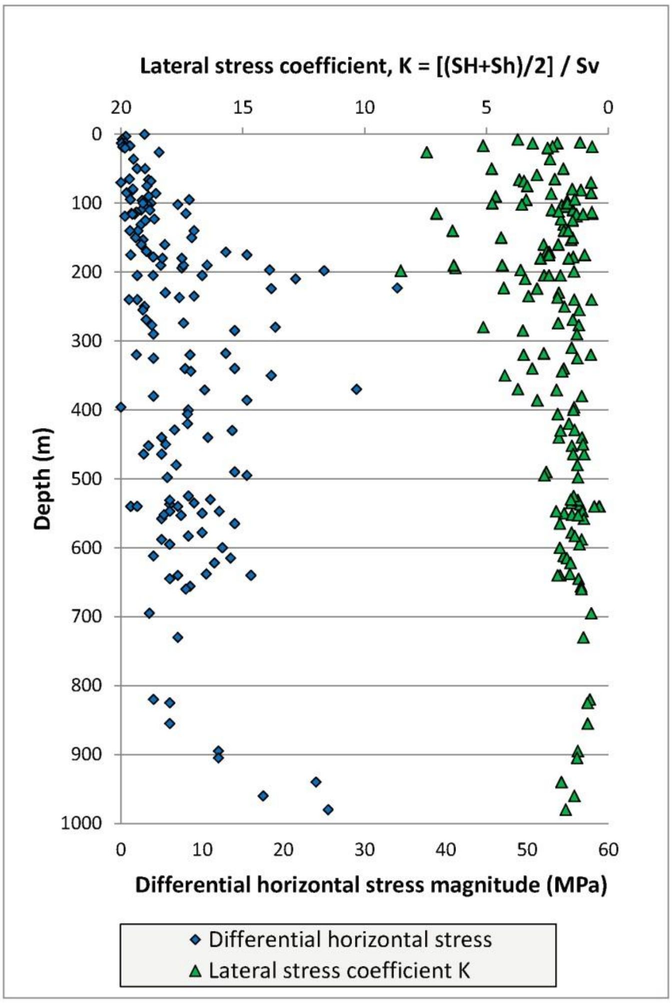

Figure 14. Lateral stress coefficient and differential horizontal stress plotted against depth, used in stress profile analysis.

The stress information shows that the Sydney Basin is overall experiencing a reverse tectonic regime; however, variations with depth are apparent (Figure 13). Conditions from surface to 200m are mixed with all three principal stress regimes represented. Strata between 200 - 400m depth are predominantly reverse; however, the zone below this is relatively mixed again, even though stress magnitude differences are lower and would indicate a more consistent trend. Conditions change to strike-slip regime abruptly from 650 to 850m, before shifting to reverse tectonics below this horizon. The significance of this is that the subsurface appears to be regionally compartmentalised with depth, and this may have led to the development of stress zones that interact with and affect formation water and gas distributions. Where possible such analysis should be carried out on a borehole-by-borehole basis or regionally; however, such level of information is not available for the basin in the public domain.

5. Discussion

Interpreted origins for the gas zonation in the Sydney basin are varied, but largely agree that the zonation exists, and commonly over-prints (i.e. 'cross-cuts') the regional stratigraphy and structure, although local variations do occur. Gas contents vary at any given depth, but the depth of the 'peak gas' horizon generally increases from north to south, as does the rank of the coal; however, the overall gas content profile with depth retains the parabolic trend. The composition of the gas shows an apparent trend with rank similar to that of thermogenic origins, with higher levels of CO_2 in the lower rank coals, and increasing amounts of methane in the higher rank coals; however, the corresponding ranks are not always in agreement with the Hunt findings (Hunt, 1979). With uplift and deformation of the basin since maximum burial in the Triassic, it is likely that significant volumes of the original thermogenic gas would not be retained in the coals, and isotope results reported from the basin show that much of the shallow gas (<800m) is biogenic. The complex compositional aspect of the gas accumulation limits the direct comparison of saturation levels between the various parts of the basin. This results in a complicated picture on the controls around *in situ* gas volumes in the basin until the effects of pore pressure from groundwater and the *in situ* stress regime are considered.

The Sydney Basin hosts hydrostatic groundwater flow to at least 500m depth (Figure 9) but this is indicated to persist to at least 800m (Burra et al., 2014; also see discussion in Section 4.1, Figure 6). Stress conditions appear most favourable to such flow above 200m depth; with more restrictions to vertical flow between 200 - 400m (Figure 12 and Figure 13). Below this horizon, horizontal stress magnitudes stabilise and differential stresses and lateral stress indicators show more consistent conditions to approximately 650m depth. At this point in the profile, the stress anisotropy decreases markedly, and the tectonic regime experiences strike-slip conditions (Figure 13). Under some conditions, this could be interpreted in favour of surface waters being able to penetrate even deeper into the subsurface; however, it is more likely that this released stress zone enables the deeper and higher pressured formation waters (and associated thermogenic gases) to migrate to lower pressures (and depths) without significant barriers. This hypothesis is supported by the abrupt appearance of (thermogenic) ethane concentrations at and below approximately 650m depth around the basin (Figure 7; Faiz et al., 2003, Burra et al., 2014). This provides further evidence that the boundary between the base of the hydrostatic zone and the uppermost reaches of the deep geopressured layer is located at ~650m in this dataset.

Conditions in this interval provide a zone of transitional environments - in terms of hydrodynamics, hydrochemistry and effective stress variation. This mixed water and altered stress zone is likely spatially extensive across the basin, as this kind of interaction is expected to occur in all regions due to effects of gravity on groundwater flow. Wide-spread mixed gas signatures reported from all areas of the Sydney Basin between the shallow biogenic and deep thermogenic gas layers (Faiz and Hendry, 2006; Thomson et al., 2008; Burra et al., 2014) provide further support for the presence of this likely setting. The mixed gas and water zone terminates at the depth where the relaxed stress conditions deteriorate and the 'unaffected' *in situ* stress and pore pressure regimes prevail. This is indicated to occur below ~850m depth in this dataset (Figure 12) that correlates well with the typical upper extent of thermogenic gas-dominated accumulations (Thomson et al., 2008; Burra et al., 2014) and the presence of higher concentrations of ethane (Figure 7).

5.1 Implications for gas distribution prediction

In situ stress characteristics and gas distributions with depth exhibit a close correlation – commonly in distinct zones. Shifts in stress attributes indicate changing gas properties, and vice versa. It is suggested that this connection is persistent in spatial extents as well, with stress regimes changing around local geological structures and sedimentological features. As a result, it is expected that gas distributions and cited depths may vary locally and be possible to map from observation of geological features present regionally. This is demonstrated to some extent in Figure 7 where the more structurally affected northern region in the vicinity of the Hunter-Mookai Thrust Belt hosts reported gas layers and volumes at noticeably shallower depths than in the central and southern parts of the basin.

More locally, deformation of strata causes changes in the stress field characteristics around geological features. Folding of strata commonly results in the increase of stress magnitudes in the limbs (compression) and the lowering of stress magnitudes in the axes (extension) (Dawson, 1999; Strout and Tjelta, 2005). Stress fields are also affected by sedimentological changes, both in terms of facies change and depth to basement (or a locally significant lower bounding surface) attributes – these have been well-documented in the Sydney Basin and other Australian coal-bearing sedimentary basins (Gale et al., 1984a, 1984b; Enever et al., 1999; Flottman et al., 2013). Changes in coal seam geometry also affect stress magnitudes, with thinner coal seams showing higher relative stress magnitudes (Enever et al., 1999) and in thick coals, the middle of the units reporting the lowest stresses (Jeffrey et al., 1997).

Gas accumulations are strongly related to hydrodynamic fluctuations (Scott, 2002; Pashin, 2007). The importance of sealing and conducive faults, dykes and other impermeable features are well-known (e.g. Pashin, 1998; Lamarre, 2003; Bell, 2006; Groshong et al., 2009; Pinetown, 2010). Coal seams in footwalls of thrust faults and syncline axes have been shown to have up to 50% higher adsorbed gas contents in the northern Sydney Basin (Burra and Esterle, 2012), and to be more outburst-prone in surrounding regions in Chinese coal mines (Cao et al., 2001).

Consequently, it appears that the relationship between regional stress fields and coal seam gas distributions may be persistent over large areas of many sedimentary basins. However, this regional relationship can be overprinted intermittently by stress perturbations around local geological features which may affect the hydrodynamic environment and associated gas accumulations. Nevertheless, qualitative estimation of likely gas trends and accumulation extents are possible from interpretation of regional geological and stress mapping, and this connection can be utilised at exploration and production stages in coal seam gas projects.

6. Conclusion

The regional stress field in the Sydney Basin is that of a predominantly compressional (reverse) regime; however, more detailed investigations depict a series of distinct stress zones with depth. Differential horizontal stress magnitudes vary between zones and changes in pore pressure gradient (effecting effective stress gradients) also play a critical role in isolating regions of possibly over-pressured strata. The stress zones appear to be strongly related to the previously documented coal seam gas zones; most likely, in relation to regulating the hydrodynamic and hydrochemical interaction within the host strata.

Regional stress patterns can be overprinted by more local perturbations, and the combinations of these create the specific local gas accumulation regime. However, overall, it is possible to use geological mapping to derive coal seam gas attributes to assist reservoir characterisation and planning of exploration targets. The widely-reported geological controls of coal seam gas distribution from many parts of the world attest to such connections being prevalent. As a result, more work should be directed towards understanding *in situ* stress characteristics and their controls on regional hydrodynamics and associated gas accumulation regimes in sedimentary basins.

Acknowledgements

This research was carried out with the support of the Australian Coal Association Research Program (ACARP) Project number C21061. Special thanks to the coal mining company assisting with data from the northern Sydney Basin, as well as Malcolm Bocking with horizontal stress data collation, and Ian Gray and Ross Seedsman for the various discussions on some of the geomechanical concepts considered in this paper. Jason Czapla and Sam Brooke-Barnett are also thanked for their advice on data validation methods. The authors would also like to thank Jack Pashin and an anonymous reviewer for their helpful comments and suggestions which resulted in an improved manuscript.

References

An, F-H., Cheng, Y-P., Wang, L., Li, W., 2013. A numerical model for outburst including the effect of adsorbed gas on coal deformation and mechanical properties. *Computers and Geotechnics* 54, 222-231. http://dx.doi.org/10.1016/j.compgeo.2013.07.013

Ambrose, W.A., Ayers, W.B.Jr., 1991. Geologic controls on coalbed methane occurrence and producibility in the Fruitland Formation, Cedar Hill Field and COAL site, San Juan Basin, Colorado and New Mexico. In: Schwochow, S.D. (Ed.), Coalbed methane of western North America: Rocky Mountain Association of Geologists Guidebook, pp. 227–240.

Anderson, M.P., 2005. Heat as a ground water tracer. Groundwater 43 (6), 951-968. doi: 10.1111/j.1745-6584.2005.00052.x

Ayers, W.B.Jr., Kaiser, W.R., 1992. Coalbed methane in the San Juan Basin of the Western United States: controls on reservoir properties and gas production. In: Beamish, B.B., Gamson, P.D.

(Eds.), Symposium on Coal Bed Methane Research and Development in Australia, 1.James Cook University, Townsville, Australia. pp. 1-30.

Back, W., Baedecker, M.J., Wood, W.W., 1993. Scales in chemical hydrogeology: a historical perspective. In: Alley, W.M. (Ed.), Regional ground-water quality, Van Nostrand Reinhold, New York, pp. 111-130.

Bell, J.S., 1996. In situ stresses in sedimentary rocks (Part 2): Applications of stress measurements. Geoscience Canada 23 (3), 135-153.

Bell, J.S., 2006. In-situ stress and coal bed methane potential in Western Canada. Bulletin of Canadian Petroleum Geology 54 (3), 197-220.

Bjorlykke, K., Hoeg, K., 1997. Effects of burial genesis on stresses, compaction and fluid flow in sedimentary basins. Marine and Petroleum Geology 14 (3), 267-276.

Blevin, J., Hall, L., Chapman, J., Pryer, L., 2007. Sydney Basin reservoir prediction study - September 2007. FrOGTech project Code: MR705.

Bocking, M.A., Weber, C.R., 1993. Coalbed methane in the Sydney Basin – Australia. Proceedings of the 1993 International Coalbed Methane Symposium, The University of Alabama / Tuscaloosa, May 17–21, 1993, pp. 1–9.

Brooke-Barnett, S., Flottmann, T., Paul, P.K., Busetti, S., Hennings, P., Reid, R., 2012. Influence of basement structures on stress regimes in the Surat and Bowen Basins, southeast Queensland. PESA Eastern Australasian Basins Symposium IV, Brisbane QLD, 10-14 September, 2012, pp 1-4.

Brown, E.T., Hoek, E., 1978. Trends in relationships between measured in-situ stresses and depth. Technical Note. International Journal of Rock Mechanics and Mining Sciences and Geomechanics Abstracts 15 (4), 211-215.

Burra, A., Esterle, J., 2012. Gas distribution and geology: a Hunter Valley example. Proceedings of the 38th Symposium on the Geology of the Sydney Basin - Advances in the study of the Sydney Basin. Pokolbin, NSW, 10-12 May, 2012.

Burra, A., Esterle, J.S., Golding, S.D., 2014. Coal seam gas distribution and hydrodynamics of the Sydney, NSW, Australia. Australian Journal of Earth Sciences 61, 427-453. doi: 10.1080/08120099.2014.912991

Bustin, R.M., 1997. Importance of fabric and composition on the stress sensitivity of permeability of some coals, Northern Sydney Basin, Australia: relevance to coalbed methane exploitation. AAPG Bull. 81 (11), 1894-1908.

Cao, Y., He, D., Glick, D.C., 2001. Coal and gas outbursts in footwalls of reverse faults. Int. J. Coal Geol. 48, 47-63.

Cercone, K.R., Deming, D., Pollack, H.N., 1996. Insulating effect of coals and black shales in the Appalachian Basin, Western Pennsylvania. Org.Geochem. 24 (2), 243-249.

Clark, I.H., Boyd, G.L., 1995. Geological controls on coalbed methane accumulations. In: Lama, R.D. (Ed.), Proceedings of the International Symposium-cum-workshop on managements and control of high gas emissions and outbursts in underground coal mines, Wollongong, NSW, Australia, pp. 369-374.

Creech, M., 1994. Some aspects of coalbed methane in the Newcastle Coalfields. Advances in the study of the Sydney Basin. 28th Newcastle Symposium, Newcastle, NSW, 15-17 April, 1994, pp. 110-117.

Dake, L.P., 1978. Fundamentals of reservoir engineering. Elsevier Scientific Publishing Company, Amsterdam. (462 pp.)

Dawson, F.M., 1999. Coalbed methane exploration in structurally complex terrain – a balance between tectonics and hydrogeology. In: Mastalerz, M., Glikson, M., Golding, S.D. (Eds.), Coalbed methane: scientific, environmental, and economic evaluation. Kluwer Academic Publishers, London. pp. 111-121.

Dolinar, D., 2003. Variation of horizontal stresses and strains in mines in bedded deposits in the eastern and Midwestern United States. In: Peng, S.S., Mark, C., Khair, A.W., Heasley, K (Eds.), Proceedings of the 22nd International Conferences on Ground Control in Mining, held at Morgantown, WV, USA, August 5-7, 2003, pp. 178-185.

Dawson, G.K.W., Esterle, J.S., 2010. Controls on coal cleat spacing. Int. J. of Coal Geol. 82, 213-218.

Draper, J.J., Boreham, C.J., 2006. Geological controls on exploitable coal seam gas distribution in Queensland. APPEA Journal 2006, 343-366.

Enever, J.R., 1993. Case studies of hydraulic fracture stress measurement in Australia. In: Hudson, J.A. (Ed.), Comprehensive rock engineering, Volume 3. Pergamon Press, Oxford. pp. 497-532.

Enever, J.R., Pattison, C.I., McWatters, R.H., Clark, I., 1994a. The relationship between in-situ stress and reservoir permeability as a component in developing an exploration strategy for coalbed methane in Australia. Presented at the SPE/ISRM Rock Mechanics in Petroleum Engineering Conference held in Delft, The Netherlands, 29-31 August 1994. SPE paper 28048.

Enever, J.R., Bocking, M.A., Clark, I., 1994b. The application of in-situ stress measurement and numerical stress analysis to coalbed methane exploration in Australia. Presented at the SPE Asia Pacific Oil & Gas Conference held in Melbourne, Australia, 7-10 November 1994. SPE paper 28780.

Enever, J.R., Henning, A., 1997. The relationship between permeability and effective stress for Australian coals and its implications with respect to coalbed methane exploration and reservoir modelling. International Coalbed Methane Symposium, Tuscaloosa, Alabama, May 12-16, 1997.

Enever, J.R., Clark, I., 1997. The current stress state in the Sydney Basin. 31st Newcastle Symposium on Advances in the Study of the Sydney Basin, Newcastle NSW Australia, April 18-20, 1997.

Enever, J.R., Glenn, R.A., Beckett, J., 1998. The stress field and structural environment of the Hunter Valley. In: Fityus, S.G., Australian Geomechanics Society (Eds.), Geotechnical engineering and engineering geology in the Hunter Valley. Conference Publications Springwood, NSW. pp.38-44.

Enever, J., Casey, D., Bocking, M., 1999. The role of in-situ stress in coalbed methane exploration. In: Mastalerz, M., Glikson, M., Golding, S.D. (Eds.), Coalbed methane: scientific, environmental, and economic evaluation. Kluwer Academic Publishers, London. pp. 297-303.

Enever, J.R., Jeffrey, R.G., Casey, D.A., 2000. The relationship between stress in coal and rock. In: North American Rock Mechanics Symposium, Girard, J. (Eds.), Pacific Rocks 2000: rock around the rim: proceedings of the fourth North American Rock Mechanics Symposium NARMS 2000 Seattle, Washington, USA, 31 July-3 August 2000. A.A. Balkema, Rotterdam; Brookfield, VT. pp. 409-414.

Enever, J.R., Lee, M.F., 2000. On the prediction of rock stress. Presented at the ISRM International Symposium, November 19 - 24, 2000, Melbourne, Australia. SPE IS paper 2000-582.

Facer, R.A., Cook, A.C., Beck, A.E., 1980. Thermal properties and coal rank in rock and coal seams of the southern Sydney Basin, New South Wales: a palaeogeothermal explanation of coalification. Int. J. of Coal Geol. 1, 1-17.

Faiz, M.M., Stalker, L., Sherwood, N., Saghafi, A., Wold, M., Barclay, S.A., Choudhury, J., Barker, W., Wang, I., 2003. Bio-enhancement of coal bed methane resources in the southern Sydney Basin. APPEA Journal 43 (1), 595-610.

Faiz, M.M., Hendry, P., 2006. Significance of microbial activity in Australian coal bed methane reservoirs - a review. Bull. of Canadian Petrol. Geol. **54**, 261-272.

Faiz, M., Saghafi, A., Sherwood, N., Wang, I., 2007a. The influence of petrological properties and burial history on coal seam methane reservoir characterisation, Sydney Basin, Australia. Int. J. of Coal Geol. 70, 193-208.

Faiz, M.M., Saghafi, A., Barclay, S.A., Stalker, L., Sherwood, N.R., Whitford, D.J., 2007b. Evaluating geological sequestration of CO_2 in bituminous coals: The southern Sydney Basin, Australia as a natural analogue. Int. J. of Greenhouse Gas Control I, 223-235.

Fertl, W. H., 1976. Abnormal formation pressures. Elsevier Scientific Publishing Company, Amsterdam. (381 pp.)

Flottman, T., Brooke-Barnett, S., Trubshaw, R., Naidu, S., Kirk-Burnnand, E., Paul, P., Busetti, S., Hennings, P., 2013. Influence of in-situ stresses on fracture stimulations in the Surat Basin, Southeast Queensland. Presented at the SPE Unconventional Resources Conference and Exhibition – Asia Pacific, held in Brisbane, Australia, 11-13 November 2013. SPE paper 167064.

Gale, W.J., Enever, J.R., Blackwood, R.L., McKay, J., 1984a. An investigation of the effect of a fault / monocline structure on the in situ stress field and mining conditions at Nattai Bulli Colliery, NSW, Australia. CSIRO Report 48.

Gale, W.J., Rawlings, C.D., Cook, C., Stone, I., Rixon, L.K., Enever, J.R., Walton, R.J., Litterbach, N., 1984b. An investigation of the stress field and its effect upon mining conditions at Tahmoor Colliery, NSW, Australia. CSIRO Report 49.

Golab, A., 2003. The impact of igneous intrusions on coal, cleat carbonate and groundwater composition. PHD Thesis, University of Wollongong, NSW, Australia.

Gray, I., 1987. Reservoir engineering in coal seams: Part 1 - the physical process of gas storage and movement in coal seams. SPE Reservoir Engineering, Volume 2 (1), February 1987.

Gray, I., 2011. Stresses in sedimentary strata, including coals, and the effects of fluid withdrawal on effective stress and permeability. 11th Underground Coal Operator's Conference, University of Wollongong and the Australian Institute of Mining and Metallurgy, 2011, 297-306. http://ro.uow.edu.au/cgi/viewcontent.cgi?article=2032&context=coal

Gray, I., Wood, J., Shelukhina, Y., 2013. Real Stress Distributions in Sedimentary Strata. Presented at the 6th International Symposium on In-Situ Rock Stress, in 20-22 August 2013, Sendai, Japan.

Groshong, R.H.Jr., Pashin, J.C., McIntyre, M.R., 2009. Structural controls on fractured coal reservoirs in the southern Appalachian Black Warrior foreland basin. J. of Struct. Geol., 31, 874-886.

Harpalani, S., Chen, G., 1992. Effect of gas production on porosity and permeability of coal. Symposium on coalbed methane research and development in Australia, pp. 67-73. James Cook University of North Queensland, Townsville, Queensland, Australia.

Haynes, M.W., 2012. Estimated stored heat in the Clarence-Moreton Basin, New South Wales: a case study in reducing uncertainties in thermal modelling. In: Mares, T. (Ed.), Eastern Australasian Basins Symposium IV. Petroleum Exploration Society of Australia, Special Publication, pp. 1-4.

Hillis, R.R., Enever, J.R., Reynolds, S., 1999. In situ stress field of eastern Australia. Aust. J. of Earth Sci. 46, 813-825.

Hillis, R.R., 2000. Pore pressure / stress coupling and its implications to seismicity. Expl. Geophys. 31, 448-454.

Hillis, R.R., Reynolds, S.D., 2003. Chapter 4 – In situ stress field of Australia. Geological Society of Australia Special Publications 22, 43-52.

Holgate, F.L., Gerner, E.J., 2010. OzTemp well temperature data. Geoscience Australia. http://data.gov.au/dataset/oztemp-well-temperature-data (Accessed 2 June 2014).

Hunt, J.M., 1979. Petroleum geochemistry and geology. W. H. Freeman and Company, Oxford. (617 pp.) ISBN 0 7167 1005 6.

Jeffrey, R.G., Enever, J.R., Henning, A., Meaney, K., Moreby, R., Doyle, R., 1997. The impact of structure and stress on permeability and gas drainage as measured at a vertical well drainage site at Dartbrook Mine. In: Doyle, R., Moloney, J. (Eds.), Symposium on safety in mines: the role of geology. 24-25 November 1997, pp. 91-103.

Katahara, K.W., 1996. Estimation of in-situ stress profiles from well-logs. SPWLA 37th Annual Logging Symposium, June 16-19, 1996. Society of Petrophysicists and Well-log Analysts. 1-14.

Kang, H., Zhang, X., Si, L., Wu, Y., Gao, F., 2010. In-situ stress measurements and stress distribution characteristics in underground coal mines in China. Eng. Geol. 116, 333-345.

Kulander, B.R., Dean, S.L., 1993. Coal-cleat domains and domain boundaries in the Allegheny Plateau of West Virginia. AAPG Bull. 81 (11), 1894-1908.

Ladeira, F.L., Price, N.J., 1981. Relationship between fracture spacing and bed thickness. J. of Struct. Geol. 3(2), 179-183.

Lamarre, R.A., 2003. Hydrodynamic and stratigraphic controls for a large coalbed methane accumulation in Ferron coals of east-central Utah. Int. J. of Coal Geol. 56, 97 – 100.

Laubach, S.E., Marrett, R.A., Olson, J.E., Scott, A.R., 1998. Characteristics and origins of coal-cleat: a review. Int. J. of Coal Geol. 35, 175-207.

Laubach, S.E., Schulz-Ela, D.D., Tyler, R., 2000. Differential compaction of interbedded sandstone and coal. Geological Society, London, Special publications 1999, 51-60. doi: 10.1144/GSL.SP.2000.169.01.04

Levine, J.R., 1993. Coalification: the evolution of coal as sources rock and reservoir rock for oil and gas. Chapter 3. In: Law, B.E., Rice, D.D. (Eds.), Hydrocarbons from coal: AAPG Studies in Geology 38, pp. 39-77.

Li, H., Shimada, S., Zhang, M., 2004. Anisotropy of gas permeability associated with cleat pattern in a coal seam of the Kushiro coalfields in Japan. Environmental Geol. 47, 45-50. doi: 10.1007/s00254-004-1125

Liu, C., 2011. Distribution laws of in-situ stress in deep underground coal mines. Proc. Eng. 26, 909-917.

Mark, C., Gadde, M., 2010. Global trends in coal mine horizontal stress measurement. *In:* Aziz, N. (Ed.), 10th Underground Coal Operator's Conference, University of Wollongong and the Australian Institute of Mining and Metallurgy, 2010, 21-39. http://ro.uow.edu.au/coal/296/

Meng, Z., Zhang, J., Wang, R., 2011. In-situ stress, pore pressure and stress-dependent permeability in the Southern Qinshui Basin. Int. J. of Rock Mech. and Min. Sci. 48, 122-131.

Middleton, M.F., Schmidt, P.W., 1982. Paleothermometry of the Sydney Basin. J. of Geophys. Res. 87(B7), 5351-5359.

Muller, R.D., Dyksterhuis, S., Ray, P., 2012. Australian palaeo-stress fields and tectonic reactivation over the past 100 Ma. Aust. J. of Earth Sci. 59 (1), 13-28.

Pashin, J.C., 1998. Stratigraphy and structure of coalbed methane reservoirs in the United States: an overview. Int. J. of Coal Geol. 35, 209-240.

Pashin, J.C., 2007. Hydrodynamics of coalbed methane reservoirs in the Black Warrior Basin: Key to understanding reservoir performance and environmental issues. Appl. Geochem. 22, 2257-2272.

Pashin, J.C., 2008. Coal as a petroleum source rock and reservoir rock. Chapter 9. In: Suarez-Ruiz, I., Crelling J. (Eds.), Applied coal petrology: the role of petrology in coal utilisation. Academic Press, Elsevier. pp. 227-262.

Pashin, J.C., 2010. Variable gas saturation in coalbed methane reservoirs of the Black Warrior Basin: implications for exploration and production. Int. J. of Coal Geol. 82, 135-146.

Pashin, J.C., Carroll, R.E., Hatch, J.R., Goldhaber, M.B., 1999. Mechanical and thermal control of cleating and shearing in coal: examples from the Alabama coalbed methane fields, USA. In: Mastalerz, M., Glikson, M., Golding, S.D. (Eds.), Coalbed methane: scientific, environmental, and economic evaluation. Kluwer Academic Publishers, London. pp. 305-327.

Pashin, J.C., McIntyre, M.R., 2003. Temperature-pressure conditions in coalbed methane reservoirs of the Black Warrior Basin: implications for carbon sequestration and enhanced coalbed methane recovery. Int. J. of Coal Geol. 54, 167-183.

Pashin, J.C., McIntyre, M.R., Mann, S.D., Kopaska-Merkel, D. C., Varonka, M., Orem, W., 2014. Relationships between water and gas chemistry in mature coalbed methane reservoirs of the

Black Warrior Basin. Int. J. of Coal Geol. 126, 92-105. http://dx.doi.org/10.1016/j.coal.2013.10.002.

Peng, S., 2007. In-situ stress and pore pressure. In: Peng, S., Zhang, J. (Eds.), Engineering geology for underground rocks. Springer Berlin Heidelberg, pp. 45-74.

Pinetown, K.L., Faiz, M.M., Saghafi, A., Stalker, L., Van Holst, J., 2008. Coal seam gas distribution in the Hunter Coalfield, Sydney Basin. PESA Eastern Australasian Basins Symposium III, Sydney NSW, 14-17 September, 2008, 399-402.

Pinetown, K., 2010. Delineation of coal seam gas domains in the Hunter Coalfield, Sydney Basin. Proceedings of 37th Symposium on the Geology of the Sydney Basin, Hunter Valley NSW, 6-7 May, 2010.

Pinetown, K., 2014. Regional coal seam gas distribution and burial history of the Hunter Coalfield, Sydney Basin. Aust. J. of Earth Sci. 61, 409-426. doi: 10.1080/08120099.2014.893539

Runnells, D.D., 1993. Inorganic chemical processes and reactions. In: Alley, W.M. (Ed.), Regional ground-water quality, Van Nostrand Reinhold, New York, pp. 131-154.

Scott, A.R., 2002. Hydrogeologic factors affecting gas content distribution in coal beds. Int. J. of Coal Geol. 50, 363-387.

Scott, A.R., Kaiser, W.R., Ayers, W.B. Jr., 1994. Thermogenic and secondary biogenic gases, San Juan Basin, Colorado and New Mexico – Implications for coalbed gas producibility. AAPG Bull. 78 (8), 1186-1209

Scott, A.R., Hamilton, D.S., 2006. Targeting Sydney-Gunnedah Basin coal seam methane exploration fairways and sweetspots based on a coalbed methane exploration model: Phase I report. NSW Department of Primary Industries Mineral Resources, Maitland, NSW.

Scott, A.R., Anderson, B., Crosdale, P., Dingwall, J., Leblang, G., 2007. Coal petrology and coal seam gas contents of the Walloon Subgroup – Surat Basin, Queensland, Australia. Int. J. of Coal Geol. 70, 209-222.

Smith, J.W., Gould, K.W., Rigby, D., 1982. The stable isotope geochemistry of Australian coals. Org. Geochem. 3, 111-131.

Smith, J.W., Pallaser, R., Rigby, D., 1992. Mechanism for coalbed methane formation. Symposium on coalbed methane research and development in Australia. James Cook University of North Queensland, Townsville, Queensland, Australia, pp. 63-73.

Solano-Acosta, W., Mastalerz, M., Schimmelmann, A., 2007. Cleats and their relation to geologic lineaments and coalbed methane potential in Pennsylvanian coals in Indiana. Int. J. of Coal Geol. 72, 187-208.

Sparks, D.P., McLendon, T.H., Saulsberry, J.L., Lambert, S.W., 1995. The effects of stress on coalbed reservoir performance, Black Warrior Basin, U.S.A. SPE paper 30734.

Staub, J.R., 1995a. Fracture analysis, diagenesis, and analysis of environments of deposition. Study of the Wollombi Brook No 1 well. Carbon Consultants International. (http://digsopen.minerals.nsw.gov.au/ DIGS report WCR270)

Staub, J.R., 1995b. Fracture analysis, diagenesis, and analysis of environments of deposition. Study of the Wybong No 1 well. Carbon Consultants International. (http://digsopen.minerals.nsw.gov.au/ DIGS report WCR264)

Stephansson, O., 1993. Rock stress in the Fennoscandian Shield. In: Hudson, J.A. (Ed.), Comprehensive rock engineering, Volume 3. Pergamon Press, Oxford. pp. 446-459

Strout, J.M., Tjelta, T.I., 2005. In situ pore pressures: What is their significance and how can they be reliably measured? Marine and Petrol. Geol. 22, 275-285.

Teufel, L.W., Rhett, D.W., Farrell, H.E., 1991. Effect of reservoir depletion and pore pressure drawdown on it situ stress and deformation in the Ekofisk Field, North Sea. In: Roegiers, J.C. (Ed.), Rock mechanics as a multi-disciplinary science: Proceedings of the 32nd US Symposium on Rock Mechanics, held at the University of Oklahoma, Norman, OK, July 1991. A. A. Balkema Publishers, Rotterdam, pp. 63-72.

Thomson, S., Hatherly, P., Hennings, S., Sandford, J., 2008. A model for gas distribution in coals of the Lower Hunter, Sydney Basin. PESA Eastern Australasian Basins Symposium III, Sydney NSW, 14-17 September, 2008.

Thomson, S., Thomson, D., Flood, P., 2014. Observations on the distribution of coal seam gas in the Sydney Basin and the development of a predictive model. Aust. J. of Earth Sci. 61, 395-407. doi: 10.1080/08120099.2014.903860

Veevers, J.J., 2000. Billion-year earth history of Australia and neighbours in Gondwanaland. GEMOC Press, North Ryde, NSW.

Yale, D.P., 2003. Fault and stress magnitude controls on variations in the orientation of in situ stress. In: Ameen, M. (Ed.), Fracture and in-situ stress characterisation of hydrocarbon reservoirs. Geological Society, London, Special Publications, 209, pp. 55-64.

Zang, A., Stephansson, O., 2010. Stress field of the Earth's crust. Springer, Heidelberg. (322 pp.)

Zhao, C., Hobbs, B.E., Muhlhaus, H.B., 1998. Analysis of pore-pressure fluid gradient an effective vertical-stress gradient distribution in layered hydrodynamic systems. Geophys. J. Int. 134, 519-526.

Zhao, S., Muller, R.D., 2001. The tectonic stress field in Eastern Australia. PESA Eastern Australasian Basins Symposium, Melbourne VIC, 25-28 November, 2001, 61-70.

Zoback, M.D., 2010. Reservoir Geomechanics. Cambridge University Press, New York. (449 pp.)

Highlights

- Gas content and composition in the Sydney Basin, Australia are zoned and cross cut basin stratigraphy and geological structure
- In situ stress, and in particular differential horizontal stress magnitudes, varies systematically with depth and controls groundwater movement
- Mixing of meteoric and geopressured fluids occurs where pore pressure exceeds effective vertical stress and strata can be fractured
- Gas and stress zone boundaries largely coincide and in situ stress regime is interpreted to be principal driver of gas distribution